PITZ EXPERIENCE ON THE EXPERIMENTAL OPTIMIZATION OF THE RF PHOTO INJECTOR FOR THE EUROPEAN XFEL

M. Krasilnikov[#], F. Stephan, G. Asova[†], H.-J. Grabosch, M. Groß, L. Hakobyan, I. Isaev, Y. Ivanisenko*, L. Jachmann, M. Khojoyan, G. Klemz, W. Köhler, M. Mahgoub, D. Malyutin, M. Nozdrin[§], A. Oppelt, M. Otevrel, B. Petrosyan, S. Rimjaem[‡], A. Shapovalov, G. Vashchenko, S. Weidinger, R. Wenndorff, DESY, Zeuthen, Germany
K. Flöttmann, M. Hoffmann, S. Lederer, H. Schlarb, S. Schreiber, DESY, Hamburg, Germany
I. Templin, I. Will, MBI, Berlin, Germany
V. Paramonov, INR, Moscow, Russia
D. Richter, HZB, Berlin, Germany

Abstract

The Photo Injector Test facility at DESY, Zeuthen site (PITZ), develops high brightness electron sources for modern free electron lasers. A continuous experimental optimization of the L-band photo injector for such FEL facilities like FLASH and the European XFEL has been performed for a wide range of electron bunch charges – from 20 pC to 2 nC – yielding very small emittance values for all charge levels. Experience and results of the experimental optimization will be presented in comparison with beam dynamics simulations. The influence of various parameters onto the photo injector performance will be discussed.

INTRODUCTION

The development of high brightness electron sources is strongly motivated by recent progress in free electron lasers based on the self-amplified spontaneous emission (SASE FELs). RF photo injectors are capable to produce electron beams with very low transverse emittance [1]. Since more than a decade the Photo Injector Test facility at DESY, Zeuthen site (PITZ), develops electron sources for modern FELs like the Free-electron Laser in Hamburg, FLASH [2], and the European X-ray Free-Electron Laser, European XFEL [3]. The stringent requirement on beam emittance for the European XFEL of 0.9 mm mrad at 1 nC bunch charge in the injector was experimentally demonstrated at PITZ [1, 4].

Besides the beam emittance a unique pulse structure has to be supported by the electron sources developed and optimized at PITZ in order to use advantage of the superconducting linac. Trains with up to 600 electron bunches and 1 μs spacing between the pulses of the train have been produced at 10 Hz repetition rate. To realize full specification for the European XFEL the bunch frequency of the photocathode laser has to be increased from 1 to 4.5 MHz. Thus, 27000 bunches per second have to be accelerated.

The pulse train structure yields an advantage for the emittance optimization at low bunch charge. The transverse emittance has been minimized for bunch charges from 0.02 to 2 nC [1, 5].

The paper gives a general overview of the PITZ accelerator and summarizes the results of the rf photo injector experimental optimization at various bunch charge levels. Beam dynamics simulations will be presented for the photo injector of the European XFEL as well as for the PITZ setup.

PITZ ACCELERATOR

A general schematic diagram of the current PITZ setup is shown in Fig. 1. The accelerator consists of a photocathode rf gun, a normal conducting booster cavity and various systems for cathode laser and electron beam diagnostics.

RF Gun

The PITZ gun is a 1.6 cell L-band normal conducting copper rf cavity with a Cs_2Te photocathode. The gun cavity is supplied with main and bucking solenoids for control and mitigation of space charge forces within electron bunches of very high density.

The rf feed of the gun is realized using a 10 MW multibeam klystron [1] which supplies the power via two waveguide arms. A T-combiner is installed in the rf gun vicinity and serves to superpose waves from these two arms to feed the gun cavity.

A phase shifter in one of the waveguides is used to match amplitudes and phases of the mixing waves. The combined wave is fed through a rotationally symmetric coaxial coupler into the rf gun. The rf feed regulation is realized on a FPGA platform based on signals from so-called 10 MW coupler [1] which measures the forward wave after the T combiner and the wave reflected from the gun cavity. The shot-to-shot rms phase jitter is ~0.1 deg, the phase slope within an rf pulse is ~0.1 deg/μs.

mikhail.krasilnikov@desy.de
† currently at INRNE, Sofia, Bulgaria
* currently at PSI, Villigen, Switzerland
§ on leave from JINR, Dubna, Russia
‡ currently at Chang Mai University, Thailand

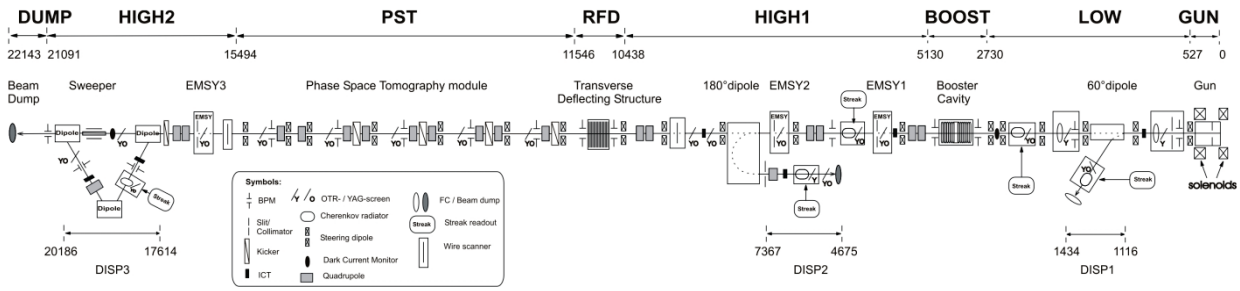

Figure 1: Schematic diagram of the PITZ electron beam line including electron gun and CDS booster cavity. Diagnostics is presented by dispersive arms (DISP1,2,3), stations with optical transition radiation and YAG screens (O/Y), and emittance measurement system stations (EMSY1,2,3). Coordinates (z positions) with respect to the cathode plane are given in mm.

The PITZ gun cavity is typically conditioned up to a peak power of ~6 MW. The maximum average rf power in the gun achieved in 2011 was 42 kW with 700 μs rf pulse duration at 10 Hz repetition rate. The typical rf pulse length used during emittance studies was up to 300 μs.

RF conditioning of the gun cavity is usually performed with a Molybdenum cathode plug, a Cs_2Te cathode can be inserted in the cavity for the beam operation without breaking the vacuum due to a vacuum load-locked cathode system.

Since 2007 the dry-ice sublimation impulse cleaning procedure is applied to all gun cavities before the rf conditioning at PITZ [6]. This resulted in a significant reduction of the dark current. The cavity prototypes 4.1 and 4.2 operated with two rf windows and a vacuum T-combiner [1] showed a dark current of 300-400 μA at ~6 MW peak power in the gun. The new configuration of the rf feed system (T-combiner filled with SF_6 and one rf vacuum window afterwards) together with a new conditioning procedure [7] resulted in even lower levels of dark current detected from cavity prototypes 3.1 and 4.3 - ~100 μA at ~6MW. Such a low dark current is very important for the superconducting linac operation. At the same time it improves the quality of electron beam measurements due to the reduction of the background signal.

Photocathode Laser

The photocathode laser system was developed by the Max-Born Institute. Currently the Yb:YAG based pulse train oscillator is capable to generate pulse trains with up to 800 micropulses and 1 μs spacing between the pulses within the train. The trains can be produced at 10 Hz repetition rate.

A temporal pulse shaper is based on 13 birefringent crystals to transform the initial short Gaussian pulse into a flattop profile with rise and fall times as short as ~2 ps and a pulse duration of 21-22 ps FWHM [8]. An optical sampling system (OSS) based on optical cross-correlation technique is used at PITZ to measure the temporal profile of the UV output pulses with a resolution of better than 1 ps. A typical temporal profile measured with the OSS is shown in Fig. 2, left plot.

An Yb:YAG regenerative amplifier and a two-stage Yb:YAG booster amplifier together with frequency conversion crystals provide UV output pulses with a wavelength of 257 nm and a maximum energy of ~10 μJ per micropulse.

Transverse pulse shaping is realized by cutting out the central part of the laser spot with a beam shaping aperture (BSA) and its consequent imaging onto the photocathode. Several plates with fixed sets of BSAs were installed in the laser beam line. This corresponds to discrete values of the laser spot diameters used in the 2011 run for the emittance optimization for various bunch charges. Currently a BSA with remotely variable diameter is installed in the PITZ optical beam line. The transverse distribution of the cathode laser is monitored with a UV sensitive CCD camera placed at a location which is optically equivalent to the real cathode position. A typical transverse distribution is shown in the right plot of Fig. 2.

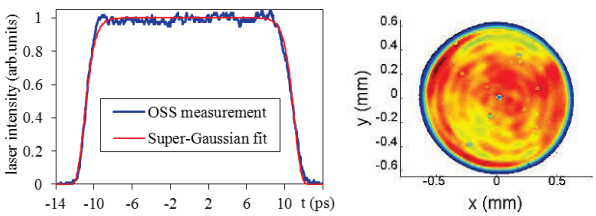

Figure 2: Photo cathode laser pulse temporal profile (left plot) and transverse distribution (right plot). The temporal profile measured with the OSS is also supplied with the Super-Gaussian fit curve: $F(t) = exp\left[-\frac{1}{2}\left|\frac{t}{10.627}\right|^{16.679}\right]$.

The cathode laser is coupled to the photocathode by means of a vacuum mirror installed slightly off the beam axis in a diagnostic cross 0.72 m downstream of the cathode plane.

CDS Booster

A booster cavity based on a cut disk structure (CDS) developed by INR (Moscow) provides a maximum final beam momentum of 24.5 MeV/c. The CDS booster is specially designed for PITZ and supports long pulse train operation at maximum peak rf power.

Beam Diagnostics

The transverse phase space of the electron beam is measured downstream of the booster at a distance of 5.74 m from the photocathode using the slit-scan technique [1, 4, 5]. The emittance measurement systems (EMSY1,2,3 – see Fig. 1) contain horizontal and vertical actuators supplied with YAG powder and optical transition radiation screens as well as slit masks with 10 μm opening made of 1 mm thick tungsten. The slit mask converts a space charge dominated electron beam into an emittance dominated beamlet which is characterized with a screen 2.64 m downstream of the slit. The part of the beam which is hitting the mask is scattered and builds a homogeneous background. By moving the slit mask transversely over the beam spot, one obtains local divergence profiles of the electron beam. The transverse phase space (x, x') can be reconstructed from the whole set of slit-scan data. The YAG screen at the EMSY position is used to measure the rms size of the whole beam σ_x. This value is typically larger than the rms size of the phase space distribution purely obtained from the slit scan $\sqrt{\langle x^2 \rangle}$ due to limiting sensitivity for very low intensity beamlets at the tails of the phase space distribution. With the assumption that the rms divergence after removing the linear covariance $\langle xx' \rangle$ from the measured phase space is close to the real uncorrelated divergence, the expression for the rms normalized (horizontal) emittance takes the form [1, 5]

$$\varepsilon_{n,x} = \beta\gamma \frac{\sigma_x}{\sqrt{\langle x^2 \rangle}} \sqrt{\langle x^2 \rangle \langle x'^2 \rangle - \langle xx' \rangle^2}\,, \qquad (1)$$

where the factor $\beta\gamma = \sqrt{\gamma^2 - 1}$ can be calculated from the relativistic Lorentz factor γ. The electron longitudinal momentum is measured by making use of a spectrometer dipole magnet and a corresponding screen in the dispersive section (DISP2 in Fig. 1). More details on the emittance measurement procedure at PITZ can be found in [1, 5].

The bunch charge is measured using integrating current transformers for a range of 0.2–2 nC, lower charges (0.02–0.2 nC) were detected using the Faraday cup in the first diagnostic cross (~0.8 m from the cathode plane).

12-bit CCD cameras are used to measure the transverse distribution of the electron beam or beamlet. In order to use the dynamic range of the 12-bit camera as much as possible the maximum intensity of the beam image is adjusted to have pixels with values of at least ~3000 but still not to be saturated (the saturation level is 2^{12}-1=4095). This intensity criterion (“3000-criterion”) is achieved by interplay of the camera gain and the number of pulses in a train, while keeping the number of pulses as low as possible to minimize the influence of the beam jitter.

BEAM DYNAMICS SIMULATIONS

In order to study the properties of high brightness electron beams in the photo injector series of beam dynamics simulations with the ASTRA code [9] were conducted. The main goal for the optimization was the transverse normalized emittance after the injector. The PITZ gun with a peak electric field of 60.6 MV/m at the cathode was used for all simulations shown below, which corresponds to the experimental conditions during the emittance optimization at PITZ. The cathode laser determines a start configuration of electrons at the cathode. It implies the noncorrelated (thermal) emittance as a lower limit for the projected emittance in the injector. On the other hand the shape and the distribution of the cathode laser contributes significantly to the structure of the space charge forces in the cathode vicinity as well as for the propagation of the space charge dominated beam. Currently a flattop temporal profile with radially homogeneous transverse distribution (Fig. 2) is the nominal laser distribution. This is significant improvement compared to the Gaussian temporal profile. More sophisticated 3D ellipsoidal photocathode laser pulses are considered to be the next essential step towards further improvements of the electron beam brightness.

1nC Case, Various Cathode Laser Temporal Profiles

Three shapes of the photocathode laser pulse were used to investigate the impact of the initial particle configuration onto the electron beam brightness after the first accelerating module (ACC1) of the European XFEL. For this setup the PITZ gun was supplied with the ACC1 consisted of 8 TESLA cavities, delivering a final beam energy of ~150 MeV. Two cylindrically shaped pulses with Gaussian and flattop temporal profiles were compared to a 3D ellipsoidal distribution [10, 11]. The last one is considered as a future upgrade of the photocathode laser at PITZ. Machine parameters for all three cases were tuned in order to produce 1 nC electron bunches of the same rms length (~2 mm). Slice parameters of the corresponding three electron bunches after the ACC1 (z = 15 m) – slice emittance and bunch current – are shown in Fig. 3.

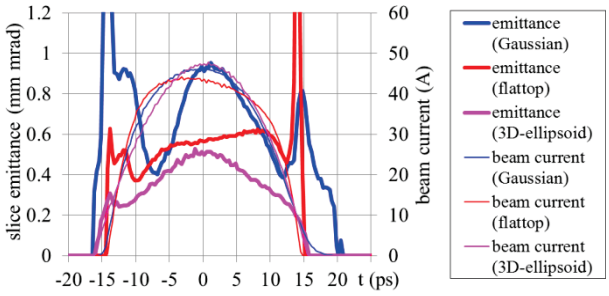

Figure 3: Comparison of three photocathode pulses – Gaussian, flattop and 3D-ellipsoidal: simulated slice emittance (left axis) and bunch current distributions along the electron bunch.

The standard definition of the beam brightness as a ratio of the peak current over the product of x- and y-emittance ($\propto I_{peak}/(\varepsilon_x \varepsilon_y)$) is not of practical use for the injector optimization. Further bunch compression increases the peak current significantly. The emittance growth due to the space charge and CSR effects reduces the brightness increase. In order to characterize the brightness of electron bunch in the photo injector slice brightness can be introduced:

$$B_{slice}(t) = \frac{I(t)}{\varepsilon_{slice,x}(t)\varepsilon_{slice,y}(t)}, \qquad (2)$$

where slice emittance $\varepsilon_{slice,x,y}(t)$ and current $I(t)$ distributions (e.g. Fig. 3) are used. Corresponding curves are shown in Fig. 4. The average slice brightness $\langle B_s \rangle$ weighted with a bunch current

$$\langle B_{slice} \rangle = \frac{\int I(t) B_{slice}(t) dt}{\int I(t) dt}, \qquad (3)$$

can be calculated to compare the performance of the high brightness photo injector. Additionally the average brightness of electron source can be used:

$$B_{injector} = \frac{I_{injector}}{\varepsilon_{n,x}\varepsilon_{n,y}} = \frac{Q \cdot NoP \cdot RR}{\varepsilon_{n,x}\varepsilon_{n,y}}, \qquad (4)$$

where the bunch charge Q, number of bunches in a pulse train NoP and the repetition rate RR are used to calculate the average current $I_{injector}$. For the nominal option of the European XFEL: $I_{injector} = 1nC \cdot 2700 \cdot 10Hz = 27\mu A$.

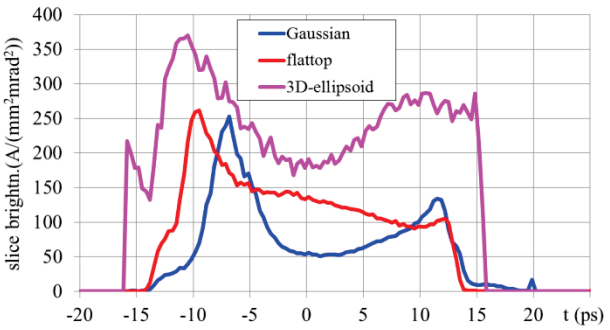

Figure 4: Comparison of three photocathode pulses – Gaussian, flattop and 3D-ellipsoidal: simulated slice brightness calculated according to equation (2) at the exit of ACC1.

A comparison of the main parameters of the electron bunches simulated using different shapes of the photocathode laser pulse are summarized in Table 1. Besides the peak bunch current and the projected transverse emittance, the average weighted slice emittance of the bunch $\langle \varepsilon_{slice,x} \rangle$, the average brightness $B_{injector}$ (equation (4)) and the average slice brightness $\langle B_{slice} \rangle$ (equation (3)) are shown in Table 1.

Table 1: Simulated electron beam properties for the European XFEL photo injector.

Parameter	Gaussian	Flattop	3D ellipsoidal
I_{peak} $[A]$	46	44	47
$\varepsilon_{n,x}$ $[mm\ mrad]$	1.05	0.63	0.43
$\langle \varepsilon_{slice,x} \rangle$ $[mm\ mrad]$	0.72	0.55	0.40
$B_{injector}$ $\left[\frac{\mu A}{(mm\ mrad)^2}\right]$	24	68	146
$\langle B_{slice} \rangle$ $\left[\frac{A}{(mm\ mrad)^2}\right]$	90	135	240

One clearly can see from the simulations that applying flattop cathode laser pulses results in 40% reduction of the projected and in ~24% reduction of average slice emittance compared to the Gaussian case. As it can be concluded from Fig. 3 the slice emittance for the flattop case is more homogeneously distributed within the bunch, whereas a rather strong bump in slice emittance is located around the center of the bunch for the Gaussian case. Further improvements on beam emittance and brightness can be obtained by using the 3D ellipsoidal pulses of the photocathode laser. A reduction of 32% in projected and ~27% in average slice emittance with respect to the flattop case was simulated for the ellipsoidal pulses. A significant improvement in the calculated average brightness of electron source and in the average slice brightness has been obtained. Applying the flattop pulses yields factor of ~2 compared to the Gaussian temporal distribution. Further factor of ~2 is obtained while using the 3D ellipsoidal shape of the photocathode laser pulse.

Flattop Temporal Profile of the Cathode Laser, Various Bunch Charges

The PITZ accelerator setup was used to simulate the beam dynamics in a photo injector for various bunch charges – from 20 pC to 2 nC. Flattop laser pulses with 21.5 ps FWHM and 2 ps rise and fall times were used for all charge levels. This corresponds to the experimental conditions at PITZ where the laser temporal pulse shaper was adjusted and fixed to deliver these settings (Fig. 2, left plot). A homogeneous radial distribution of the transverse distribution of the laser intensity was assumed for all simulation cases. Other machine parameters – main solenoid peak field, transverse rms laser spot size, rf gun launch phase – were varied to minimize the projected normalized transverse emittance at the location of the first emittance measurement station (EMSY1, z = 5.74 m from the cathode plane). The CDS booster peak field was fixed around 20 MV/m and the maximum acceleration phase was used, delivering a final longitudinal momentum of

the electron beam of 23 MeV/c, which corresponds to the experimental conditions.

Results of the beam dynamics optimization are shown in Fig. 5 where the simulated projected emittance is plotted as a function of the rms laser spot size for various bunch charges. These curves were obtained by laser spot size variation around the optimum value for each charge case whereas the other machine parameters were fixed.

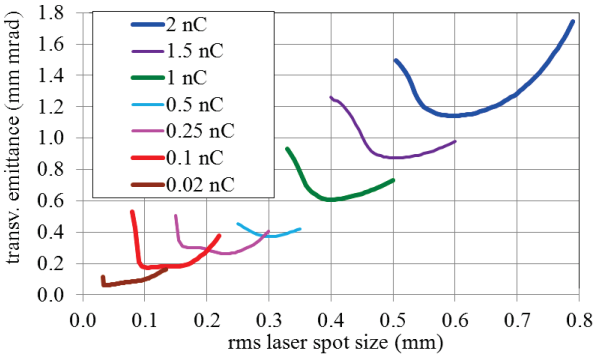

Figure 5: Simulated transverse projected normalized emittance versus rms laser spot size for various values of the bunch charge.

The slice brightness (2) is plotted in Fig. 6 for the optimum cases of the different charges.

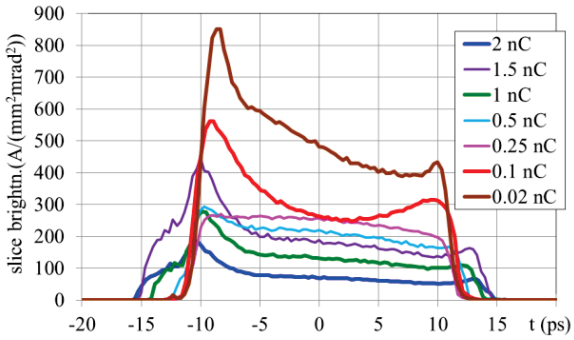

Figure 6: Simulated slice brightness (2) for various values of the bunch charge.

Summarizing plots of the projected and average slice emittance as well as the weighted average slice brightness (3) are shown in Fig. 7 as functions of the bunch charge. One should notice that for these simulations results the cathode laser pulse duration was fixed at 21.5 ps (FWHM). This implies a significant modification of the space charge effect during emission from the cathode with the bunch charge increase. Thus, the aspect ratio $c\sigma_t/\sigma_{x,y}$ of the optimum laser pulse (or an initial electron bunch) is ~50 for 0.02 nC whereas this ratio is ~3 for the case of 2 nC. The reduction of the emittance with the bunch charge decrease is stronger than the corresponding current reduction and significantly higher average slice brightness was simulated for low charges (Fig. 7).

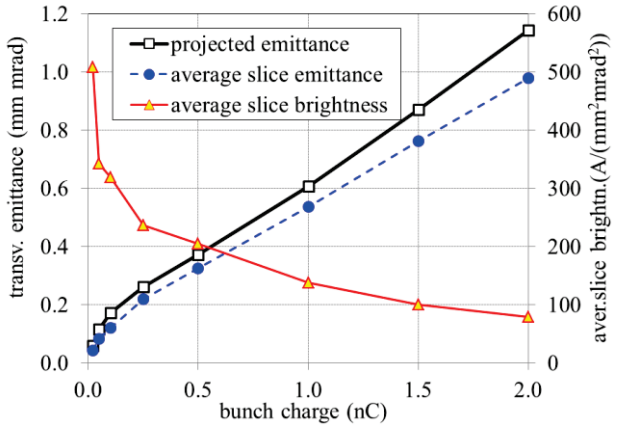

Figure 7: Simulated projected and average slice emittance as function of the bunch charge. The average slice brightness is plotted at the right axis.

1nC Flattop Case, Sensitivity on Machine Parameters

The dependence of the simulated emittance on the machine parameters for 1 nC bunch charge and the flattop cathode laser profile was studied in order to establish the experimental optimization procedure. The influence of the main tuning parameters – main solenoid peak field, laser rms spot size and the rf gun launch phase are illustrated in Table 2. The errors (detuning) of the main solenoid peak field (current) and the rms spot size of the cathode laser pulse are given in relative values to the optimum point, whereas the launch phase errors are calculated in degrees.

Table 2: Simulated emittance growth due to machine parameters errors.

Machine parameter	**Relative emittance growth**		
	5%	**10%**	**30%**
Main solenoid peak field (relative)	0.2%	0.3%	0.6%
Cathode laser rms spot size (relative)	6%	9%	13%
RF gun launch phase (deg)	1.0 deg	1.6 deg	3.0 deg

The main solenoid current is the most sensitive machine parameter for the emittance optimization. The emittance minimum is expected around a main solenoid current of 400 A, therefore a step of 1–2 A is typical for the experimental procedure of the emittance minimization. The optimum cathode laser rms spot size of ~0.4 mm was found for 1 nC beam dynamics simulations.

A 100 μm step in the laser diameter (rms size multiplied by factor 4) was recommended for the practical optimization.

EXPERIMANTALLY OPTIMIZED EMITTANCE

The general experimental procedure for the minimization of the transverse projected emittance is described in details in [1]. For each level of the bunch charge several BSAs (laser rms spot sizes) were tested to deliver the smallest emittance. Also the rf gun launch phase was varied for higher bunch charges – 1 and 2 nC. For each point (BSA, gun phase) the main solenoid current was scanned to find its optimum value yielding the minimum value of the geometrical mean $\sqrt{\varepsilon_{n,x}\varepsilon_{n,y}}$ of the measured rms normalized emittance. The gun gradient was fixed to the maximum available at that moment (a peak electric field at the cathode of ~60.6 MV/m) yielding a maximum mean momentum of the electron beam of ~6.7 MeV/c measured downstream of the gun in the low energy dispersive arm (DISP1 in Fig. 1). The CDS booster was operated at the maximum acceleration phase at the peak field yielding a maximum mean momentum of the electron beam of ~25 MeV/c.

Emittance versus Bunch Charge

The measured projected normalized xy- emittance (geometric mean of the values for the x and y plane) as a function of the laser rms spot size at the photocathode is shown in Fig. 8 for the various bunch charges. The curves for 1 and 2 nC include minimum emittance values of two gun phases – 0 deg and +6 deg w.r.t. to the gun phase of the maximum mean momentum gain (MMMG) of the electron beam [5].

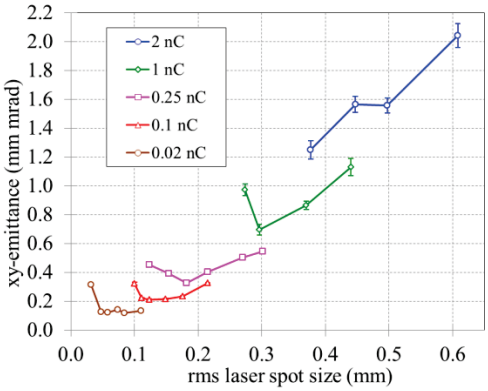

Figure 8: Measured rms normalized transverse emittance as a function of the laser spot size at the cathode for various bunch charges. The statistical error bars (see [1] for details) are included in the graph but small statistical error bars are hidden behind markers in the plot.

The measured minimum emittance is shown in Fig. 9 as a function of the bunch charge together with corresponding simulated optimized data. The average electron source brightness $B_{injector}$ calculated using (4) for the simulated and measured data is plotted as well. The duty cycle (27000 electron bunches per second) of the European XFEL injector was applied for these calculations. There is a general agreement in the measured and simulated emittance dependencies. The simulated brightness has a local maximum between 0.25 and 0.5 nC and a local minimum around 0.1 nC which could be explained by the above mentioned space charge modifications while the bunch charge is varied. The measured average brightness has an absolute maximum around 0.25 nC and decays for lower charges. This could be (at least partially) explained by that fact that for low charges longer pulse trains were integrated in order to obtain better signal to noise ratio (to satisfy the above mentioned intensity criterion). Additionally, the rms spot size of the electron beam at the position of slits for the emittance measurements is significantly smaller for lower bunch charges ($\sqrt{\sigma_x\sigma_y} \approx 70\ \mu$m for 0.02 nC, whereas $\sqrt{\sigma_x\sigma_y} \approx 300\ \mu$m for 1 nC). The resolution of the measuring system for transverse distribution electron beams comes close to its systematic limitation for lower charges yielding higher values of the measured beam (beamlet) sizes. Also, the position jitter of the electron beam contributes much more to the local divergence measurements for low charge bunches. All these factors result in an overestimation of the measured emittance and, thus, in a strong underestimation of the average brightness.

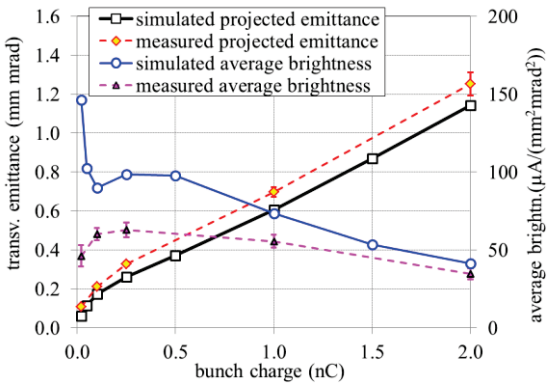

Figure 9: Measured and simulated rms normalized transverse emittance as a function of the bunch charge. The measured and simulated average brightness (4) is plotted at the right axis.

Results of the experimental optimization of the PITZ photo injector for different bunch charges are summarized in Table 3. The gun phase in the table is given with respect to the phase of maximum mean momentum of the electron beam. Values of the rms laser spot size and emittance are calculated as the geometrical mean of corresponding parameters measured in *x* and *y* planes.

It should be noticed that despite rather good and consistent agreement on measured and simulated optimum emittance values there are several discrepancies between the experimentally obtained optimum machine parameters and those expected from the beam dynamics simulations [1]. So, the optimum rms laser spot size for

1 nC is 0.3 mm in experiment whereas the simulations yield 0.4 mm. Also the simulated optimum rf gun phase is around the phase of the MMMG, the experimental optimization results in an +6 deg offset.

Table 3: Experimentally optimized photo injector parameters

Bunch charge (nC)	Gun phase (deg)	Main solenoid current (A)	RMS laser spot size (mm)	XY-emittance (mm mrad)
0.02	0	388	0.085	0.108
0.1	0	394	0.123	0.212
0.25	0	393	0.182	0.328
1	+6	396	0.296	0.697
2	+6	395	0.377	1.251

The scaling of the emittance dependence on the bunch charge (Fig. 9) is strongly dependent on the conditions of the optimization. Namely, the laser transverse spot size was tuned for each charge value whereas the temporal profile remained a flattop with 21.5 ps FWHM (Fig. 2, left plot). This modifies the space charge effect (transverse, longitudinal and their coupling) while the bunch charge varies. Also the PITZ setup (position of the main solenoid, CDS booster and locations of the emittance measurement station) was optimized for the nominal bunch charge of 1 nC and was fixed for all optimized bunch charges. Indeed, a full optimization including the photo injector layout should result in lower emittance values for various bunch charges.

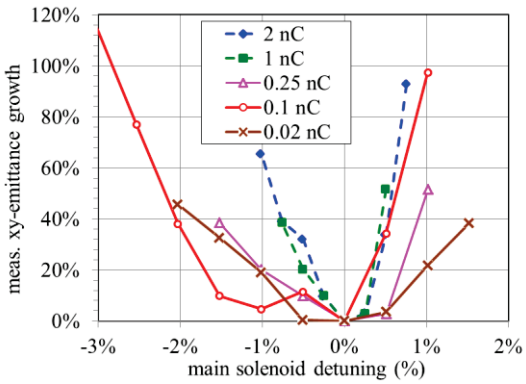

Figure 10: Measured emittance growth as a function of the main solenoid current detuning. For absolute values of emittance and solenoid current see Table 3.

Emittance versus Main Solenoid Current

Measurements of the beam emittance as a function of the main solenoid current are basic measurements for each emittance optimization step. Typical curves of these dependencies are shown in Fig. 10 where the relative emittance growth is plotted versus the main solenoid detuning from the optimum solenoid current. Values of the optimum solenoid current can be found in Table 3 as well as absolute values of the measured emittance ($\sqrt{\varepsilon_{n,x} \cdot \varepsilon_{n,y}}$).

As it was expected from simulations the emittance dependence on the main solenoid current is rather strong and it is stronger for higher charges (1 and 2 nC). The low charge curves are more flat, the measurement uncertainty is higher in this case due to systematic limitations of the measurement system [1].

Emittance Versus Homogeneity of the Cathode Emission Area

In order to study the role of the cathode emission area homogeneity, a dedicated test has been performed [1]. After the emittance optimization, the photocathode #110.2 which was actively used in the operation period was replaced by a fresh cathode #11.3. Before and right after the cathode exchange, the QE maps of both cathodes were measured [1]. The old cathode has a rather large QE inhomogeneity especially in the centre area. This is an indication of an active cathode usage especially for the low charge optimization when small laser spot sizes and long pulse trains were applied. The new cathode showed a very homogeneous QE map [1]. Because of the necessity to change the BSA for the QE-map measurements, it was not possible to perfectly reproduce the laser transverse distribution after the cathode exchange. Reinsertion of the laser BSA of 1.2 mm diameter resulted in a more homogeneous laser transverse distribution. It is hard to separate the effect of the more homogeneous QE map of the fresh cathode from the improved laser transverse distribution but the homogeneity of the emission which is presented as a convolution of the QE map and the laser transverse distribution in Fig. 11 was significantly improved.

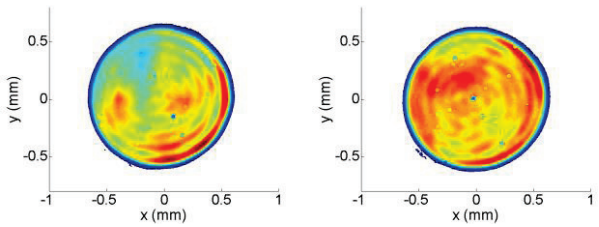

Figure 11: Emission area of the used cathode #110.2 (left) and the fresh cathode #11.3 (right) obtained from a convolution of the measured QE-map and laser transverse distribution measured with a UV sensitive CCD camera placed at a location which is optically equivalent to the real cathode position.

The best machine setup for the nominal 1 nC bunch charge (laser rms spot size of ~0.3 mm and gun phase of +6 deg) was applied and the main solenoid current scan for the best emittance was performed for each case. The corresponding experimental curves are shown in Fig. 12. The optimum solenoid current was found to be 396 A for both cases. The final reproducibility check for this point resulted in a geometrical mean of 0.762±0.017 mm mrad

for the used cathode #110.2 and 0.661±0.033 mm mrad for the fresh cathode #11.3. The corresponding optimum phase space measured before and after the cathode exchange is shown in Fig. 13. Despite rather small visual differences in the measured electron beam distributions, the phase space measured after the cathode exchange is more symmetric, having sharper edges. The observed x-y asymmetry remains but is being modified.

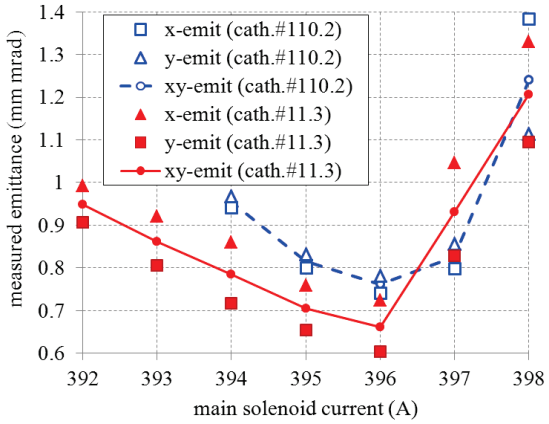

Figure 12: Measured transverse projected emittance as a function of the main solenoid current obtained for the used cathode #110.2 and the fresh cathode #11.3.

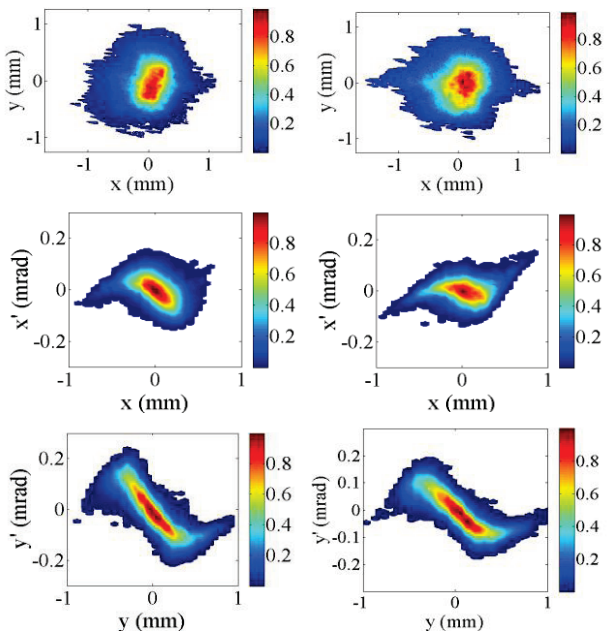

Figure 13: Measured transverse distribution of electron beam at EMSY1 (upper row), horizontal (middle row), and vertical phase space (bottom row) for a bunch charge of 1 nC. The left column of plots corresponds to the left emission pattern in Fig. 11, the right column those with the right one.

As it was discussed in [1] the optimum conditions for 1 nC (namely rather small rms spot size of the laser pulse) correspond to a strong space charge effect at the photocathode. That is why the difference in the emission pattern (Fig. 11) is probably reduced by the space charge effect leading to a saturation of the hot spots in the transverse distributions. But still the improvements in the electron beam structure are in good agreement with the effect of emission area homogenization.

Core Emittance

The emittance measurement procedure at PITZ is supposed to be as conservative as possible. This means that, as much as possible electron beam related signal has to be collected and involved in the phase space reconstruction. The emittance values are obtained from these measurements without any assumption concerning the particle distribution function. This approach results in a conservative estimation of the rms emittance values and the phase space distributions, which contain a significant part of beam particles far distant from the phase space center. Those outlying particles are not expected to play a significant role in the later FEL lasing processes but have a substantial impact on the emittance values. So, one can apply a charge cut procedure to the measured raw phase spaces in order to study the structure of the core emittance and the role of the beam halo. The charge cut is performed on the measured phase space distributions by discriminating phase space areas with intensities lower than an introduced threshold. The resulting core emittance measured for various bunch charges is shown in Fig. 14. The charge cut was applied to the corresponding measured optimum x- and y- phase spaces for each bunch charge.

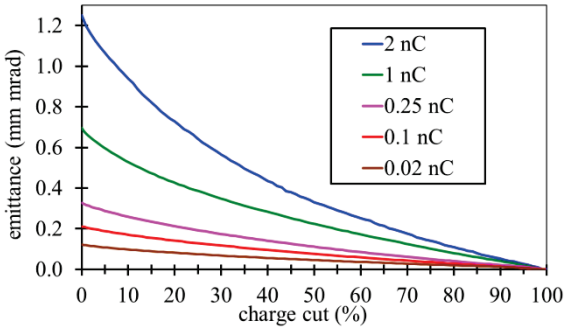

Figure 14: Measured core xy-emittance for different charges as a function of the charge cut. A charge cut of 0% corresponds to the emittance values from the raw phase space with full beam signal taken into account (for the data see Tab. 3).

CONCLUSIONS AND OUTLOOK

This paper has summarized the PITZ experience in the experimental optimization of high brightness electron sources for modern SASE FELs like FLASH and the European XFEL. A challenging pulse train structure is supported in order to use advantages of the superconducting linac.

The transverse projected normalized emittance of the electron beam was experimentally optimized for a wide range of bunch charges - from 0.02 to 2 nC. Low values of the measured emittance were obtained for the whole bunch charge range. The measured average brightness of the electron source has shown a reduction for low bunch charges (<0.1 nC) whereas the beam dynamics simulations predict its growth. This discrepancy could be due to features of the measurement procedure at low bunch charges. More studies have to be performed for this parameter range.

Further development of electron beam diagnostics is on-going at PITZ towards extensive studies on slice properties of electron bunch. The time resolved beam measurements should be realized using an rf deflector (RFD in Fig. 1). Improvements on emittance measurements for low bunch charges (~10 pC) are of great interest as well.

The cathode laser is one of the vital components for a good photo injector performance. A flattop laser temporal profile with short rise and fall time was used at PITZ to minimize the emittance of space charge dominated electron beams. The role of the transverse homogeneity of the photoemission pattern was studies experimentally. As a next step in the photocathode laser improvements a 3D ellipsoidal pulse shaping is now in preparation for PITZ [11].

REFERENCES

[1] M. Krasilnikov et al., "Experimentally minimized beam emittance from an L-band photoinjector", PRST-AB, 15, 1000701 (2012).

[2] W. Ackermann et al., Nature Photon. 1, 336 (2007).

[3] M. Altarelli et al., DESY, Hamburg Report No. DESY 2006-097, 2007.

[4] F. Stephan et al., Phys. Rev. ST Accel. Beams 13, 020704 (2010).

[5] S. Rimjaem et al., Nucl. Instrum. Methods Phys. Res., Sect. A 671, 62 (2012).

[6] F. Stephan et al., "New experimental results from PITZ", in Proceedings of the 24th Linear Accelerator Conference, Victoria, British Columbia, Canada, 2008.

[7] I. Isaev et al., "Conditioning status of the rf gun at PITZ", TUPS030, FEL2013.

[8] I. Will and G. Klemz, Opt. Express 16, 14922 (2008).

[9] K. Flöttmann, ASTRA particle tracking code http://www.desy.de/~mpyflo/

[10] M. Khojoyan et al., "Beam dynamics optimization for the high brightness PITZ photo injector using 3D ellipsoidal cathode laser pulses", TUPS036, FEL2013.

[11] M. Krasilnikov et al., "Development of a photo cathode laser system for quasi ellipsoidal bunches at PITZ", TUPS039, FEL2013.